J. Amer. Soc. Hort. Sci. 150(1):34–41. 2025. https://doi.org/10.21273/JASHS05448-24

Biomass and Yield in *Solanum lycopersicum* Expressing a Synthetic Photorespiration Pathway

Laura Dougherty
US Department of Agriculture, Agricultural Research Service, Beltsville Agricultural Research Center, Genetic Improvement for Fruits & Vegetables Laboratory, Beltsville, MD 20705, USA

Bret Cooper
US Department of Agriculture, Agricultural Research Service, Beltsville Agricultural Research Center, Soybean Genomics and Improvement Laboratory, Beltsville, MD 20705, USA

James Bunce
US Department of Agriculture, Agricultural Research Service, Beltsville Agricultural Research Center, Adaptive Cropping Systems Laboratory, Beltsville, MD 20705, USA

Bryan Vinyard
US Department of Agriculture, Agricultural Research Service, Northeast Area Statistics Group, Beltsville, MD 20705, USA

John Stommel
US Department of Agriculture, Agricultural Research Service, Beltsville Agricultural Research Center, Genetic Improvement for Fruits & Vegetables Laboratory, Beltsville, MD 20705, USA

Keywords. crop yield, metabolic efficiency, metabolite profile, photosynthetic efficiency, tomato, transgenes

Abstract. Considerable interest exists in improving the efficiency of photosynthesis and photorespiration to increase crop yields that will address growing world food needs. The current study investigated whether a novel synthetic photorespiratory pathway demonstrated to reduce photorespiratory metabolic energy demands and increase plant vegetative biomass in model species could boost tomato crop yield, notably yield of marketable fruit. The tomato cultivar Moneymaker was transformed with a synthetic photorespiration pathway construct containing a *Cucurbita maxima* malate synthase (MS) gene and a *Chlamydomonas reinhardtii* glycolate dehydrogenase (CrGDH) gene targeted to the chloroplast, with a plastid glycolate-glycerate translocator 1 (*PLGG1*) hairpin interference construct targeting the native photorespiratory pathway. Plants of seven T_2 generation lines from independent transformation events expressed the MS and CrGDH transgenes, while having at least 3-fold reduction of native *PLGG1* expression relative to non-transformed Moneymaker. Plants from transformed lines were larger and exhibited up to 63% increased biomass in comparison with the Moneymaker control. The number of fruit was similarly greater (1.4- to 4.2-fold) in modified plants; however, average individual fruit weights were significantly less for all but one line. Among transformed lines, larger fruited lines had the lowest biomass, while the smaller fruited lines had the highest biomass. Values for VC_{max} and J_{max} derived from CO_2 assimilation curves were statistically similar or lower in transformants relative to the control. Metabolic profiles obtained from high-performance liquid chromatography mass spectrometry (HPLC-MS) analysis revealed increases in forms of inactivated auxin. Principal component analysis of metabolite profiles separated transformants into two groups distinguished by total biomass and fruit size. Observed increases in plant biomass in transformed lines suggests that energy savings were realized from reduced photorespiration but were directed toward vegetative growth. Further studies to balance vegetative vs. reproductive biomass and exploit higher fruit counts observed in transformants may be beneficial for enhanced fruit yield.

The world population is predicted to reach 9.6 billion people by 2050 (Tripathi et al. 2019) and peak to 10.3 billion people by mid-2080 (United Nations 2024). As the population continues to grow, the demand for food increases. Agricultural advancements during the Green Revolution and development of high-yielding crop varieties has been critical for food production growth (Evenson and Gollin 2003). However, it is estimated that to meet the demand of the growing population, crop yield needs to increase by 70% by 2050 (FAO 2009). At current rates, crop production will not be able to meet this demand increase (Long et al. 2015). Crop yields are beginning to plateau and researchers have turned their attention to improving photosynthesis and photorespiration to increase yield (Evans 2013; Faralli and Lawson 2020; Maurino 2019; Price et al. 2011).

Photosynthesis converts light energy to chemical energy in plants. Ribulose 1,5 bisphosphate carboxylase/oxygenase (RuBisCO) binds CO_2 to carry out the Calvin-Benson cycle, a C_3 carbon fixation pathway in many plants including tomato (Raines 2022). The specificity of RuBisCO to bind CO_2 decreases in high temperatures and drought conditions leading to increased O_2 binding (Ehleringer et al. 1991). When RuBisCO binds O_2,

Received for publication 30 Sep 2024. Accepted for publication 11 Nov 2024. Published on 27 Jan 2025.
Mention of trade names or commercial products is solely for the purpose of providing specific information and does not imply recommendation or endorsement by the US Department of Agriculture.
J.S. is the corresponding author. E-mail: john.stommel@usda.gov.

photorespiration occurs, resulting in the formation of 2-phosphoglycolate (2PG) (Maurino 2019). The two-carbon 2PG short-circuits the C_3 reductive photosynthetic carbon cycle. Carbon in 2PG, however, is salvaged in a C_2 cycle that converts 2PG to glycolate in the chloroplast. In a series of reactions, glycolate moves to the peroxisome through the chloroplast glycolate-glycerate transporter PLGG1 and is transformed to glycine, which is transported to the mitochondrion and converted to serine, which is sent back to the peroxisome and transformed to 3-carbon glycerate, which moves finally back to the chloroplast to reenter the C_3 cycle after phosphorylation (South et al. 2018). This carbon salvage is an energy-expensive process requiring ATP and NADPH (Peterhansel et al. 2010) and multiple organelles. It is estimated that every fourth reaction of RuBisCO is an oxygenase reaction. The oxygenase activity of RuBisCO results in a 50% extra energy cost for photosynthesis (Peterhansel et al. 2010). Hence, photorespiration can reduce crop biomass production by 20% to 50% (South et al. 2019).

Strategies to reduce photorespiration and therefore increase photosynthetic efficiency have been explored (Zhu et al. 2020). One strategy is to optimize RuBisCO to reduce oxygenase activity (Jin et al. 2023; Whitney et al. 2011; Yadav and Mishra 2020). Hybrid engineered RuBisCO containing the large subunit from one species and the small subunit from another species have been tested (Zhang et al. 2011). Another strategy is to bypass/divert native photorespiration in plants (Kebeish et al. 2007; Shen et al. 2019; South et al. 2019). The *Escherichia coli* glycolate catabolic pathway was introduced to *Arabidopsis thaliana*, allowing the plant to directly convert glycolate to glycerate in the chloroplast by introducing glyoxylate carboligase (GCL), tartronic semialdehyde reductase, and glycolate oxidase enzymes (Kebeish et al. 2007). Transgenic *Arabidopsis* grew faster than controls and had more shoots and biomass (Kebeish et al. 2007). In cucumber, the same pathway increased seed yield by 33.4% and biomass by 59% in low CO_2 conditions (Chen et al. 2019). In a different study, glycolate catabolic cycle enzyme genes for glycolate oxidase (GO), MS, and catalase (CAT) were expressed in *Arabidopsis* chloroplasts (Maier et al. 2012). Again, transgenic *Arabidopsis* expressing all three genes had more biomass, higher photosynthetic rates, and changes in glycine/serine ratios (Maier et al. 2012). In tobacco, similar synthetic pathways have been analyzed with and without a hairpin RNAi construct silencing the gene for the glycolate-glycerate transporter (PLGG1) that shuttles glycolate from the chloroplast to the peroxisome in photorespiration (South et al. 2019). Both pathways increased dried biomass. A third pathway (AP3) consisting of *Cucurbita maxima* MS, and *Chlamydomonas reinhardtii* glycolate dehydrogenase with and without the PLGG1 RNAi was reported in tobacco (South et al. 2019). These constructs with and without the PLGG1 RNAi increased biomass 10% and 24%, respectively, in a field trial (South et al. 2019).

Given the promising biomass increase results in the AP3 pathway with PLGG1 RNAi in the tobacco model plant system using synthetic photorespiration pathways (South et al. 2019), we sought to determine if the addition of synthetic photorespiration pathway in the indeterminate 'Moneymaker' tomato plants could increase plant biomass and fruit yield. In 2023, seven transgenic T_2 'Moneymaker' lines, and nontransgenic 'Moneymaker' controls were grown and evaluated over the course of the field season. Photosynthetic parameters, aboveground biomass, fruit quality, and fruit yield were evaluated.

Materials and Methods

Plant construct and transformation. The indeterminate fresh market tomato (*Solanum lycopersicum*) cultivar Moneymaker (MM) was transformed with a synthetic photorespiration pathway construct designated AP3 with *plgg1* RNAi (AP3-RNAi) generously provided by the Ort Laboratory (South et al. 2019). The construct contains a *Cucurbita maxima* MS gene and a *Chlamydomonas reinhardtii* glycolate dehydrogenase (CrGDH) gene targeted to the chloroplast, with a plastid glycolate-glycerate translocator 1 (*PLGG1*) hairpin interference construct. Plant transformations were performed following published protocols (Van Eck et al. 2019). *Agrobacterium tumefaciens* strain LBA4404 (Intact Genomics, St. Louis, MO, USA) was used for transformation and 2 mg/L BASTA was used for selection. Rooted seedlings were acclimated in soil for 1 week under a light rack then moved to the greenhouse (75 °F/70 °F, 16 h daylight). Individual transformation events from different cotyledons were considered independent lines.

Transgene line confirmation and seed extraction. DNA from T_0 lines were extracted from leaf tissue using the DNeasy plant kit (Qiagen, Germantown, MD, USA). Polymerase chain reaction (PCR) was performed using Platinum II Taq Hot-Start PCR master mix with platinum GC enhancer (Thermo Fisher Scientific, Waltham, MA, USA) to confirm the presence of the transgenes and selection marker (Supplemental Table 1). PCR conditions were as follows: 94 °C 2 min, followed by 35 cycles of 94 °C 15 s, 63 °C 15 s, 68 °C 1:15 min, and a final 2-min extension at 68 °C. Bands were visualized on a 1.5% agarose gel infused with GelRed (Biotium Inc., Fremont, CA, USA) on a ChemiDoc system (Bio-Rad, Hercules, CA, USA). For subsequent generations and plant screening, DNA was extracted using a rapid extraction protocol (Edwards et al. 1991) with slight modifications. Briefly, leaf samples were ground using a metal bead, and mixed with extraction buffer. Samples were centrifuged and the supernatant was transferred to a new tube and mixed with equal amounts of isopropanol and centrifuged again. The isopropanol was removed, and the pellet was washed with 80% ethanol and centrifuged again. All liquid was removed, and the pellet was air dried for 5 min before the pellet was resuspended in 1xTE buffer. T_0 lines were advanced to the T_2 generation via self-pollination with testing at respective generations for the transgene as described previously.

Field prep/planting. In preparation for the field trial, a 128-plug tray was planted for each T_2 line and nontransgenic control on 1 May 2023, and grown in the greenhouse. The last week of May, all seedlings were screened to confirm they were transgenic as described above. Plants were handplanted in 3-ft-wide raised beds covered with black plastic, 23 inches apart in a research field (39.29523–76.930175) in Beltsville, MD, 9 Jun 2023, equipped with drip irrigation. In the field, the five replications of each line were planted in a randomized order. Six-foot cedar stakes were placed every two plants, and field string was tied between stakes to encourage upright growth. Fertilization and irrigation followed standard cultural practices established for the Mid-Atlantic region (Rutgers University 2024).

RNA isolation, cDNA synthesis/qPCR. During the field season, young leaf tissue from three field plants per line, per replication were collected and flash frozen in liquid nitrogen. The leaf samples were ground in liquid nitrogen and RNA was

extracted using the GeneJET Plant RNA Purification kit (Thermo Fisher Scientific) according to the manufacturer's protocol.

cDNA was synthesized using 1 mg of total leaf RNA with the ProtoScript First Stand cDNA Synthesis Kit (New England BioLabs, Ipswich, MA, USA) with oligo dT primers according to manufacturer's protocol. The finished cDNA product was diluted 2x with distilled H_2O for downstream use. Quantitative PCR (qPCR) was completed for each leaf sample in triplicate using iTaq Universal SYBR Green Supermix (Bio-Rad) on a CFX-96 machine (Bio-Rad). A two-step qPCR (95 °C 30 s, 95 °C 10 s, 60 °C 30 s × 39) with a melt curve (65 to 95 °C, 5 s at 0.5 °C intervals) was used. Expression analysis was completed using Bio-Rad CFX Maestro software. β-Tubulin was used for a reference gene (Changwal et al. 2021), while expression of transgenes *MS*, *CrGDH*, and native *PLGG1* (Solyc08g076290) were quantified. Primers are listed in Supplemental Table 1.

CO_2 assimilation. CO_2 assimilation curves were obtained for three field plants, per line, per replication over the course of 9 d (31 Jul 2023–8 Aug 2023) between the hours of 10:00 AM and 3:00 PM using the CIRAS-3 DC CO2/H2O Gas Analyzer (PP-Systems, Amesbury, MA, USA), CO_2 levels were ramped from 100 ppm to 1500 ppm under 1500 $\mu mol \cdot m^{-2} \cdot s^{-1}$ light. Using the R package "Plantecophys" (Duursma 2015) the rate of maximum velocity of carboxylation (Vc_{max}) and maximum pathway flux (J_{max}) values were calculated for each line per replication.

Fruit quality and weights. Vine-ripened red tomato fruits were randomly picked from all lines and replications and weighed. Five fruits were blended, and juice was extracted through cheese cloth. Total soluble solids (Brix) and titratable acidity (citric acid) were measured using the PAL-BX|ACID meter, program 3 (ATAGO, Tokyo, Japan) and pH was measured using S47 SevenMulti™ dual meter pH/conductivity (Mettler Toledo, Columbus, OH, USA).

Harvest and biomass measurements. Aboveground biomass was harvested from the field over the course of 17 d (18 Sep 2023–5 Oct 2023) for all lines and replications. All fruits were harvested from the plants and counted. Biomass (stems and leaves) was dried over the course of at least 1 month on greenhouse benches. After drying, all biomass weights were recorded.

Metabolic analysis samples. T_2 seeds of transgenic lines MM-1, MM-2, MM-3, MM-4, MM-5, MM-6, and MM-C were grown in a growth chamber at 26 °C, 60% relative humidity, 800 $\mu mol \cdot m^{-2} \cdot s^{-1}$ light with 14 h light/10 h dark cycles. Three weeks after germination, the plants were screened by PCR for the presence of transgenes. By 4 weeks after germination, PCR+ transgenic plants produced secondary leaves while the slower-growing MM-C had only primary leaves of similar size. Leaf samples were taken from the first internode leaf for MM-C and the second internode leaves for the transgenics. In total 0.18 g of leaves (10–12 1-cm disks using a 1-cm cork-borer) from two plants were combined to form one replicate. Five replicates were prepared for each transgenic line and MM-C.

Mass spectrometry. The leaves were homogenized in a tube containing 0.5-mm glass beads and 0.7 mL water and 0.7 mL phenol/chloroform. Two matrix blanks with solutions but without tissue were also created. The tubes were centrifuged at 16,000 g_n for 30 min. The aqueous layer was reserved and recentrifuged. The supernatant was transferred to a glass vial and dried under vacuum. The residues were resuspended in 120 µL 0.1% formic acid; 10 µL was taken from each tube and combined to create a quality control (QC) sample.

Five-microliter injections of the samples, blanks, and QC were used in the subsequent procedure. Injections were separated on a 150 × 2.1-mm Hypersil GOLD VANQUISH HPLC column with 1.9-µm particles (Thermo Fisher Scientific) at 40 °C coupled to a Vanquish HPLC pump (Thermo Fisher Scientific) controlling a 10-min linear gradient from 0% to 95% acetonitrile and 0.1% formic acid at a flow rate of 0.2 mL per minute. Eluent was electrosprayed at 3.5 kV positive polarity into an Exploris 240 mass spectrometer (Thermo Fisher Scientific). The instrument settings and methods for nontargeted mass spectrometry acquisition are described (Cooper et al. 2024). The samples were analyzed in both positive and negative ion mode and the data were analyzed separately with Compound Discoverer version 3.3 (Thermo Fisher Scientific) as previously described (Cooper and Yang 2024). The software compared observed MS^2 spectra to reference spectra in the mzCloud and NIST 2023 MSMS High-Resolution libraries. The software performed a one-way analysis of variance (ANOVA) to estimate compound chromatographic peak area statistical differences and used the Benjamini and Hochberg method to estimate the false discovery rate. Filtering of results was performed to limit background ions, to include normalized areas, to require MS^2 of preferred ions, for Adj. P values < 0.05 for any transgenic line, and for library match scores ≥ 70. Results were examined by hand and discarded if the chromatographic peaks were substandard or if the MS^2 identifying spectrum did not fall within the assigned chromatographic peak area.

Statistical methods. For biomass, fruit yield and fruit weight analysis from five replicate plots were examined for each transgenic line and the control. The number of individual plants composing each replicate plot varied from plot to plot and line to line (Supplemental Table 2). The observed data values used to represent each replicate plot were average biomass per plant, average number of fruits per plant, and average weight per fruit. Graphical examination (Boxplots) of among-replicate variability for each cultivar indicated likely heterogeneity of variability across lines for the Moneymaker cultivar; confirmed by significant likelihood ratio test comparing heterogeneous variance models to the homogeneous model. One-way line ANOVA models were fit using the gls function in the nlme R package; specifying a variance group (i.e., vg) factor assigning lines that exhibited among-replicate variability differing from variability of other lines by greater than 4x magnitude to a different group, facilitated using the dplyr and tidyverse R packages. The variance group factor was specified as weights = varIdent(form=~1|vg) in the gls function. Pairwise means comparisons among lines were obtained using the emmeans, multcomp, and multcompView packages in R version 4.3.2. For fruit quality analysis of pH, titratable acidity and Brix of the five replicate plots were conducted in JMP® Pro version 17.0 (SAS Institute Inc., Cary, NC, USA). Means, standard errors, and mean comparisons using the Student's t test were performed.

Results

Transgenic line development and gene expression. Seven transgenic AP3-RNAi Moneymaker lines were produced for this study. The AP3-RNAi construct was selected based on the high yield increases (24%) observed in tobacco field trials (South et al. 2019). There were visible differences among the lines early in the field season (Fig. 1). Notably, MM-2, MM-4, MM-5, MM-6, and MM-7 exhibited increased branching and axillary

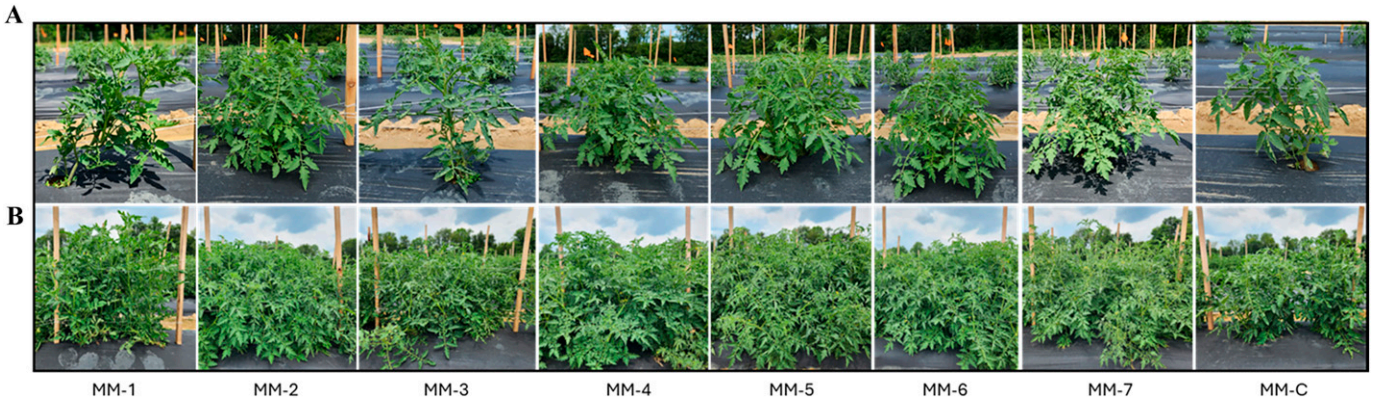

Fig. 1. Representative pictures of young transgenic and control lines used in this study. (**A**) Plants shown 24 d after field planting (64 d after seeding). (**B**) Plants 44 d after field planting (84 d after seeding).

shoot development. Height measurements were taken weekly from 21 Jun 2023 through 27 Jul 2023 to assess vegetative growth before onset of fruit set. Lines MM-1, MM-2, MM-4, MM-5, MM-6, and MM-7 exhibited greater plant height in comparison with the control (Supplemental Fig. 1).

Each line expressed the MS and CrGDH transgenes, while having at least 3-fold reduction of native *PLGG1* expression when compared with the control (Fig. 2). In the synthetic photorespiratory pathway that we introduced into transformed tomato plants, the reaction catalyzed by CrGDH precedes the MS reaction (South et al. 2018). Lines MM-1, MM-3, and MM-7 had higher CrGDH transgene expression than MS transgene expression, while MM-2, MM-4, MM-5, and MM-6 had higher MS transgene expression than *CrGDH* transgene expression.

Biomass and fruit yield. At harvest, the aboveground biomass and fruit were collected. MM-C had the lowest biomass weight per plant at 532 g, while MM-2 had the highest biomass weight at 965 g. The larger fruited lines MM-C, MM-1, and MM-3 had the lowest biomass, while the smaller fruited lines had the highest biomass (Fig. 3A, Supplemental Table 3). Overall comparisons of MM-C to the transgenic AP3-RNAi lines revealed a 12.2% to 63.0% increase in biomass for the transgenic lines (Supplemental Table 4). Biomass values for MM-1 and MM-3 were higher than the control (12.2% and 12.8%, respectively), but differences were not significant.

There were clear differences in fruit weight among the lines. The Moneymaker control (MM-C) had the largest fruit, averaging 69.9 g per fruit (n = 598) followed by MM-3 at 57.7 g (n = 498) and MM-1 with 39.9 g (n = 487). The remaining lines MM-2 (n = 576), MM-4 (n = 606), MM-5 (n = 563), MM-6 (n = 499), and MM-7 (n = 542) all had small fruit weighing an average of 17 g, 17.4 g, 15.7 g, 17 g, and 17.9 g, respectively (Supplemental Fig. 2). Fruit weights of these small-fruited lines were 25% of the control line fruit weights. Only line MM-3 was not statistically different from the control, while all the others weighed significantly less (Fig. 3B, Supplemental Table 5). The larger fruited lines MM-C, MM-1, and MM-3 had the lowest biomass, while the smaller fruited lines had the highest biomass (Fig. 3A, Supplemental Table 3).

When evaluating the average number of fruits per plant, trends similar to those for vegetative biomass were observed.

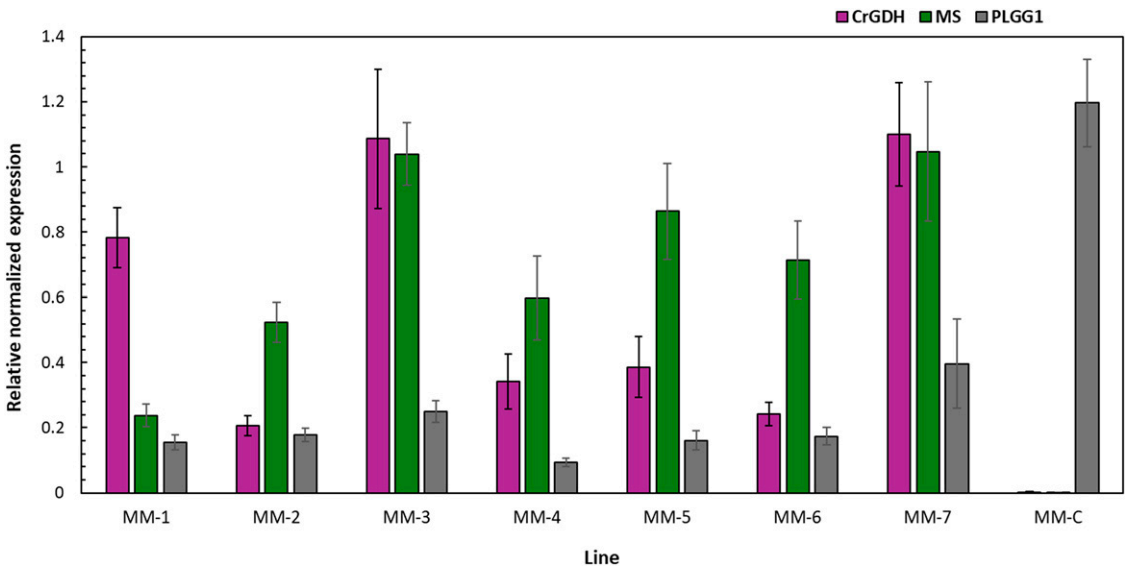

Fig. 2. Transgene and native *Plgg1* expression profiles. Expression profiles of transgenes *CrGDH* and *MS*, and native *PLGG1* in young field leaves. The error bars represent standard error of the mean.

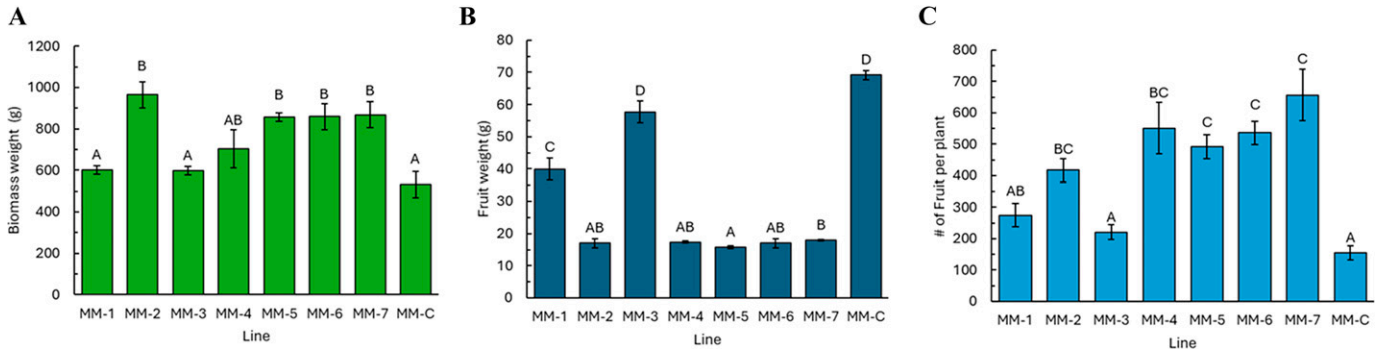

Fig. 3. Harvest data. (**A**) Average biomass per plant. (**B**) Average fruit weight and (**C**) average number of fruits per plant. The error bars represent the standard error of the means. Different letters represent statistically significant differences between lines ($P < 0.05$).

The larger fruited lines MM-C, MM-1, and MM-3 had the least fruit per plant (n = 155, 274, and 221, respectively) while the smaller fruited lines had the greatest number of fruit per plant with MM-7 having the highest fruit count, averaging 657 fruit per plant (Fig. 3C, Supplemental Table 6). When compared with MM-C, only lines MM-1, MM-3, and MM-7 had a greater total fruit weight (2.1%, 19.1%, and 9.8%, respectively) (Supplemental Table 7). The smaller fruited lines MM-2, MM-4, MM-5, and MM-6 had large reductions in total fruit weight (−33.8%, −10.5%, −27.9%, and −14.9%, respectively). Despite significant increases in fruit per plant in the small-fruited transgenics, only MM-7 had greater total fruit weight per plant in comparison with MM-C.

Fruit quality characteristics. Fruit pH, total soluble solids, and titratable acidity were measured to determine if the AP3-RNAi construct altered fruit quality traits. Variation in fruit pH across transformed lines and the control was low, ranging from 4.21 to 4.32. Lines MM-2 and MM-5 had significantly lower fruit pH than MM-C (Fig. 4A). For the total soluble solids, MM-1 Brix values were significantly lower compared with MM-C (4.78% and 5.56%, respectively), while lines MM-4 and MM-7 were significantly higher (6.68% and 6.64%, respectively) (Fig. 4B). MM-4 (0.72) and MM-7 (0.77) also had higher titratable acidity than MM-C (0.52) (Fig. 4C). Although there were significant differences between MM-C and many of the transgenic lines, differences were not consistent across lines for individual fruit quality attributes and could not be directly attributed to the effects of the AP3-RNAi construct.

CO_2 assimilation. The CO_2 curve measurements were used to calculate the Vc_{max} and J_{max} parameters used to characterize photosynthetic potential (Fig. 5). The Vc_{max} values were significantly different between lines MM-1, MM-4, MM-6, MM-7, and MM-C. Overall MM-C had the highest Vc_{max} (122.2), whereas MM-1 had the lowest (89.1). Similar trends were observed for J_{max}, with MM-1, MM-4, MM-5, MM-6, and MM-7 having significantly lower values when compared with MM-C. Again MM-C had the highest value (247.4) and MM-6 had the lowest (163.0). VC_{max} and J_{max} were significantly lower relative to the control in all the transgenic lines expect for MM-2 and MM-3 ($P < 0.05$).

Metabolic data. We performed nontargeted tandem mass spectrometry on metabolite extracts from leaves of transgenics and controls to assess potential biochemical differences between the lines. There were 2778 compound ions identified in negative ion mode and 2054 identified in positive ion mode. Principal component analysis of negative ion mode metabolites revealed clustering differences (Fig. 6). MM-1 samples clustered separately from the others. MM-C and MM-3 clustered together while lines MM-2, MM-4, MM-5, and MM-6 clustered with each other (MM-7 was not analyzed). These cluster groups correlated with the physical measurements whereby MM-2, MM-4, MM-5, and MM-6 all had greater plant biomass, higher numbers of fruit, and lower fruit weight. Because the transgenics express *CrGDH* and *MS*, we examined the metabolomics data for potential changes in glycolate, glyoxylate, and malate. We did not observe ions for glycolate or glyoxylate above background. Three isomers of malate were observed but none significantly changed (Supplemental Table 8). Because the transgenics also have reduced *PLGG1* expression, it is possible that this led to decreased glycerate pools as shown by South et al. (2019) in AP3-RNAi transgenic tobacco, but we did not observe decreased glycerate (Supplemental Table 8). Thus, these metabolomics data do not

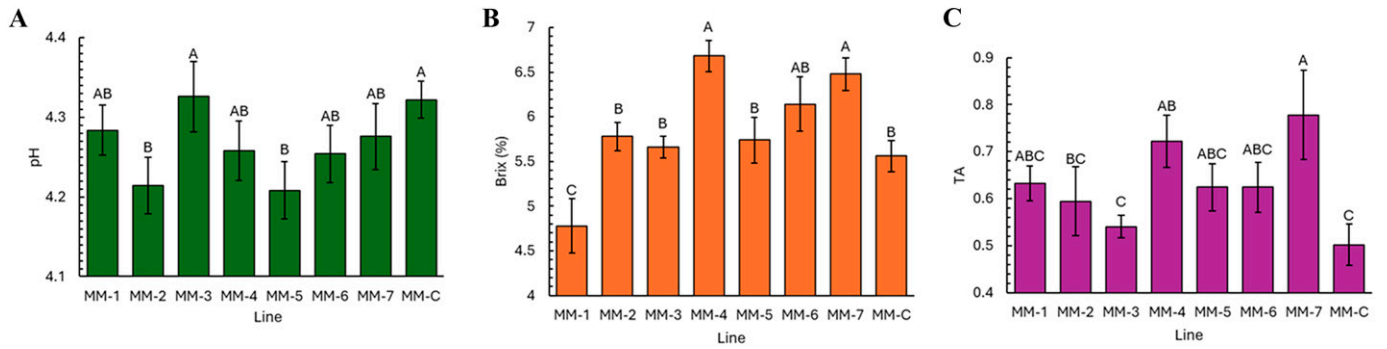

Fig. 4. Fruit quality evaluation. (**A**) Average fruit juice pH, (**B**) fruit juice total soluble solids, and (**C**) titratable acidity (TA). Error bars represent the standard error of the means. Letters represent significance differences between lines ($P < 0.05$).

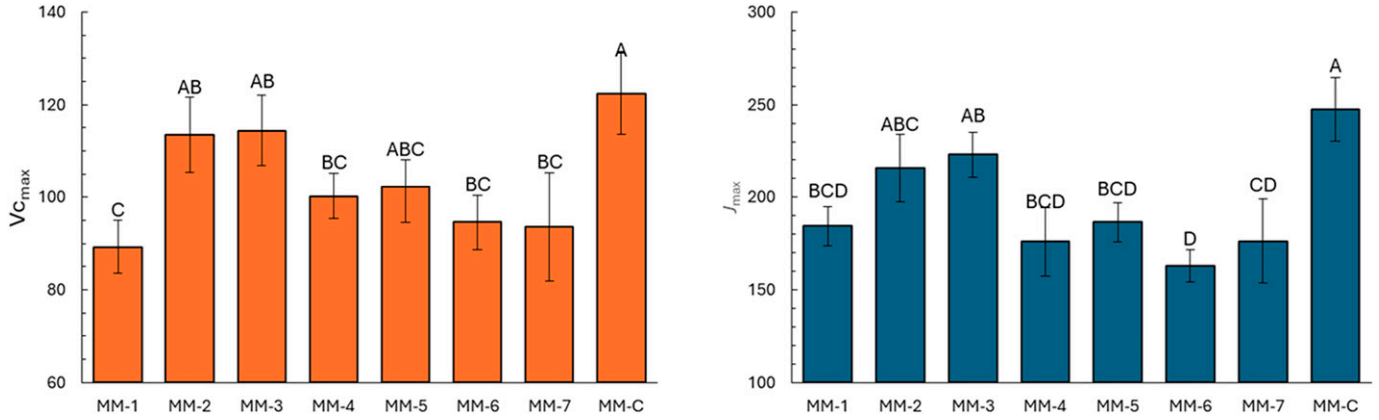

Fig. 5. Photosynthesis parameters obtained based on CO_2 assimilation curves. (**A**) Vc_{max} is the maximum rate of RuBisCO carboxylase activity and (**B**) J_{max} is the maximum rate of photosynthetic electron transport. The error bars represent standard error of the mean. Letters represent significant differences between lines ($P < 0.5$).

sufficiently provide evidence for enhanced carbon flux through the engineered pathways as previously described (South et al. 2019). Nevertheless, we did observe near 2-fold or greater increases of oxidized indole-3-acetic acid (oxIAA) and oxidized indole-3-acetic acid-aspartate (oxIAA-ASP) in all transgenics plants (Supplemental Table 8). oxIAA and oxIAA-ASP are the main inactivated forms of the plant hormone auxin (Hayashi et al. 2021). Thus, we interpret the increased amounts of inactivated auxin as evidence of the hormonal regulation of former, rapidly growing young leaves.

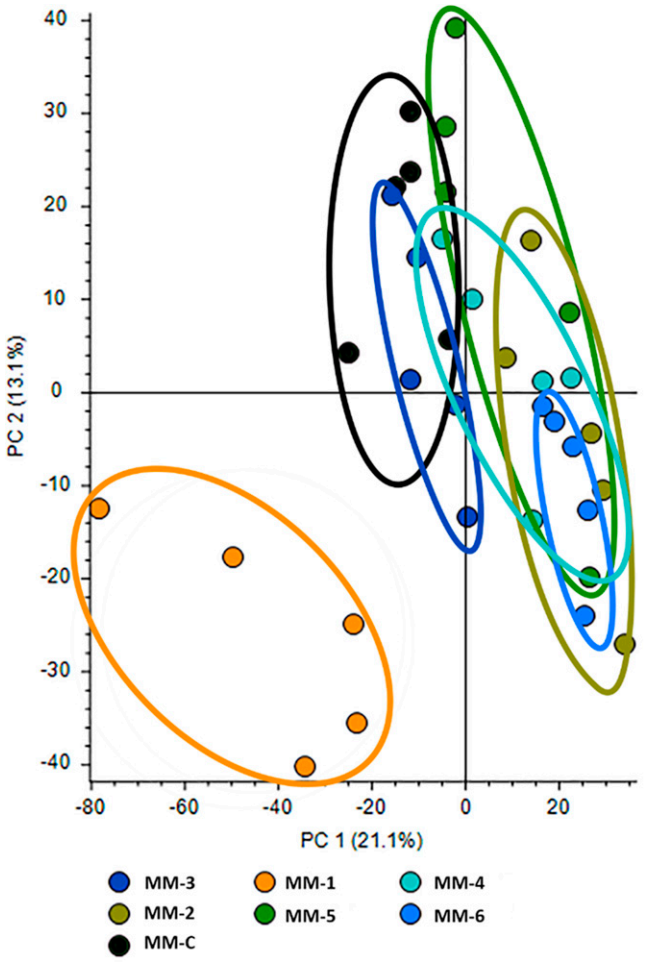

Fig. 6. Principal component analysis plot of metabolic profiles for Moneymaker transgenic and control lines. The circles indicate groupings of the five replicates.

Discussion

The indeterminate Moneymaker transgenic lines could be classified into two main groups (Figs. 3A, 4A). Group 1 contains the larger fruited/low biomass lines MM-1 and MM-3. These lines were more similar to nontransgenic Moneymaker with respect to fruit weight, fruit number, and plant biomass. Group 2 consists of the smaller weighted fruit lines MM-2, MM-4, MM-5, MM-6, and MM-7. These plants had higher biomass and fruit per plant than the nontransgenic Moneymaker. The transgene expression levels did not exhibit consistent relationships with observed biomass weight or fruit per plant. For example, lines MM-3 (from group 1) and MM-7 (from group 2) have similar transgene expression profiles and very different biomass weights and fruit per plant. Conversely, only lines MM-1, MM-3, and MM-7 had greater total fruit weight relative to controls and had increased expression of *CrGDH* relative to *MS* (Supplemental Table 7, Fig. 2).

The transgenic lines expressing AP3-RNAi all had higher biomass weight and fruit per plant when compared with the nontransgenic control. The reduction in native *PLGG1* expression from the AP3-RNAi construct is expected to reduce native transport of glycolate from the chloroplast to the peroxisome, thus increasing glycolate as a substrate for transgenic *CrGDH* in the chloroplast. A study in rice containing a photorespiratory bypass called "GOC bypass" exhibited increased biomass yield and photosynthetic efficiency (Shen et al. 2019). Similarity, AP3-RNAi tobacco plants produced increased biomass yield and photosynthetic efficiency (South et al. 2019) and *Arabidopsis* expressing a glycolate oxidative cycle exhibited increased biomass (Maier et al. 2012).

In the tomatoes, the VC_{max} and J_{max} were significantly lower in our transgenic tomato lines expect for MM-2 and MM-3 (Fig. 5). Our CO_2 assimilation curves were taken in full sunlight and atmospheric CO_2 levels. Harley and Sharkey (1991), concluded that under conditions of high light and carbon availability, synthesis of sink compounds (sucrose and starch) may not keep pace with production of phosphorylated intermediates in the

Calvin cycle, leading to an imbalance of phosphate that may ultimately limit photosynthesis (Harley and Sharkey 1991; Peterhansel et al. 2010). This may explain why some transgenics had lower photosynthetic capacities based on V_{Cmax} and J_{max} values. Although we did not measure mesophyll conductance, small changes in conductance can limit photosynthesis (Flexas et al. 2007, 2008), therefore it is possible that the mesophyll conductance between lines may have differed and may have contributed to the differences in V_{Cmax} and $J_{max.}$ There is also evidence that V_{Cmax} is related to leaf nitrogen and phosphorous levels (STITT 1991). Although nutrient deficiency symptoms were not observed, rapid growth may have stressed nutrient availability.

Although our metabolomics analysis did not provide evidence for enhanced carbon flux through the pathway engineered from the AP3-RNAi construct, we observed increased amounts of inactivated forms of the plant hormone auxin, which regulates leaf growth. Thus, it is likely that the increased carbon flux affected hormonal regulation, accelerating leaf development. Although we did not measure auxin in the meristematic tissue, we suspect that the increased abundance of axillary shoots in the transgenic plants will correlate with increased auxin at the meristem. Thus, our results with AP3-RNAi transformed tomato expressing a synthetic photorespiration pathway may be explained by changes arising from rapid growth from additional carbon that was directed to the meristem of the indeterminate tomato. It is possible that the transgenic meristem became a sink for carbon, upsetting the sink-source balance, which resulted in smaller fruit size (Stitt 1991). Further development of this system in tomato may necessitate transformation of determinate tomatoes but also manipulating hormonal growth regulation so the carbon moves into fruits rather than leaves.

Photorespiration intermediates are involved in other metabolic pathways in plants (Novitskaya et al. 2002). The reduced expression of the *PLGG1* transporter, may have also limited the native photorespiration pathway. The potential reduction of native photorespiration and therefore its intermediates, could be involved in the growth differences and metabolic profiles in the transgenic lines. Such investigations were beyond the goals of our initial study to determine if the addition of a synthetic photorespiration pathway in tomato could increase plant biomass and fruit yield.

The AP3-RNAi synthetic pathway increased plant biomass and fruit count in Moneymaker tomatoes. However, fruit weight was significantly less for all but one line in comparison with the Moneymaker control. Field plants were allowed to grow freely with no fruit pruning or pruning of axillary shoots. Reduction of reproductive and vegetative sinks via such pruning, may result in enhanced marketable fruit yields in tomato expressing our synthetic photorespiratory pathway. Further studies to optimize fruit size would be beneficial to balance vegetative vs. reproductive biomass and exploit observed 1.4 to 4.2-fold higher fruit counts observed in AP3-RNAi lines.

References Cited

Changwal C, Shukla T, Hussain Z, Singh N, Kar A, Singh VP, Abdin MZ, Arora A. 2021. Regulation of postharvest tomato fruit ripening by endogenous salicylic acid. Front Plant Sci. 12:663943. https://doi.org/10.3389/fpls.2021.663943.

Chen Z, Kang X, Nie H, Zheng S, Zhang T, Zhou D, Xing G, Sun S. 2019. Introduction of exogenous glycolate catabolic pathway can strongly enhances photosynthesis and biomass yield of cucumber grown in a low-CO2 environment. Front Plant Sci. 10:702. https://doi.org/10.3389/fpls.2019.00702.

Cooper B, Yang R. 2024. An assessment of AcquireX and Compound Discoverer software 3.3 for non-targeted metabolomics. Sci Rep. 14(1):4841. https://doi.org/10.1038/s41598-024-55356-3.

Cooper B, Yang R, Campbell KB. 2024. Indole alkaloid production by the halo blight bacterium treated with the phytoalexin genistein. Phytopathology. 114(6):1196–1205. https://doi.org/10.1094/PHYTO-11-23-0445-R.

Duursma RA. 2015. Plantecophys - An R package for analysing and modelling leaf gas exchange data. PLoS One. 10(11):e0143346. https://doi.org/10.1371/journal.pone.0143346.

Edwards K, Johnstone C, Thompson C. 1991. A simple and rapid method for the preparation of plant genomic DNA for PCR analysis. Nucleic Acids Res. 19(6):1349. https://doi.org/10.1093/nar/19.6.1349.

Ehleringer JR, Sage RF, Flanagan LB, Pearcy RW. 1991. Climate change and the evolution of C4 photosynthesis. Trends Ecol Evol. 6(3):95–99. https://doi.org/10.1016/0169-5347(91)90183-X.

Evans JR. 2013. Improving photosynthesis. Plant Physiol. 162(4):1780–1793. https://doi.org/10.1104/pp.113.219006.

Evenson RE, Gollin D. 2003. Assessing the impact of the green revolution, 1960 to 2000. Science. 300(5620):758–762. https://doi.org/10.1126/science.1078710.

FAO. 2009. High level expert forum-how to feed the world in 2050. Economic and Social Development, Food and Agricultural Organization of the United Nations, Rome, Italy Plant Cell, Tissue and Organ Culture.

Faralli M, Lawson T. 2020. Natural genetic variation in photosynthesis: An untapped resource to increase crop yield potential? Plant J. 101(3):518–528. https://doi.org/10.1111/tpj.14568.

Flexas J, Diaz-Espejo A, Galmes J, Kaldenhoff R, Medrano H, Ribas-Carbo M. 2007. Rapid variations of mesophyll conductance in response to changes in CO_2 concentration around leaves. Plant Cell Environ. 30:1284–1298. https://doi.org/10.1111/j.1365-3040.2007.01700.x.

Flexas J, Ribas-Carbó M, Diaz-Espejo A, Galmés J, Medrano H. 2008. Mesophyll conductance to CO_2: Current knowledge and future prospects. Plant Cell Environ. 31(5):602–621. https://doi.org/10.1111/j.1365-3040.2007.01757.x.

Harley PC, Sharkey TD. 1991. An improved model of C3 photosynthesis at high CO2: Reversed O2 sensitivity explained by lack of glycerate reentry into the chloroplast. Photosynth Res. 27(3):169–178. https://doi.org/10.1007/BF00035838.

Hayashi K, Arai K, Aoi Y, Tanaka Y, Hira H, Guo R, Hu Y, Ge C, Zhao Y, Kasahara H, Fukui K. 2021. The main oxidative inactivation pathway of the plant hormone auxin. Nat Commun. 12(1):6752. https://doi.org/10.1038/s41467-021-27020-1.

Jin K, Chen G, Yang Y, Zhang Z, Lu T. 2023. Strategies for manipulating Rubisco and creating photorespiratory bypass to boost C_3 photosynthesis: Prospects on modern crop improvement. Plant Cell Environ. 46(2):363–378. https://doi.org/10.1111/pce.14500.

Kebeish R, Niessen M, Thiruveedhi K, Bari R, Hirsch H-J, Rosenkranz R, Stäbler N, Schönfeld B, Kreuzaler F, Peterhänsel C. 2007. Chloroplastic photorespiratory bypass increases photosynthesis and biomass production in *Arabidopsis thaliana*. Nat Biotechnol. 25(5):593–599. https://doi.org/10.1038/nbt1299.

Long SP, Marshall-Colon A, Zhu X-G. 2015. Meeting the global food demand of the future by engineering crop photosynthesis and yield potential. Cell. 161(1):56–66. https://doi.org/10.1016/j.cell.2015.03.019.

Maier A, Fahnenstich H, Von Caemmerer S, Engqvist MK, Weber AP, Flügge U-I, Maurino VG. 2012. Transgenic introduction of a glycolate oxidative cycle into *A. thaliana* chloroplasts leads to growth improvement. Front Plant Sci. 3:38. https://doi.org/10.3389/fpls.2012.00038.

Maurino VG. 2019. Using energy-efficient synthetic biochemical pathways to bypass photorespiration. Biochem Soc Trans. 47(6):1805–1813. https://doi.org/10.1042/BST20190322.

Novitskaya L, Trevanion SJ, Driscoll S, Foyer CH, Noctor G. 2002. How does photorespiration modulate leaf amino acid contents? A dual approach through modelling and metabolite analysis. Plant Cell Environ. 25(7):821–835. https://doi.org/10.1046/j.1365-3040.2002.00866.x.

Peterhansel C, Horst I, Niessen M, Blume C, Kebeish R, Kürkcüoglu S, Kreuzaler F. 2010. Photorespiration. Arabidopsis Book. 8:e0130. https://doi.org/10.1199/tab.0130.

Price GD, Badger MR, von Caemmerer S. 2011. The prospect of using cyanobacterial bicarbonate transporters to improve leaf photosynthesis in C_3 crop plants. Plant Physiol. 155(1):20–26. https://doi.org/10.1104/pp.110.164681.

Raines CA. 2022. Improving plant productivity by re-tuning the regeneration of RuBP in the Calvin–Benson–Bassham cycle. New Phytol. 236(2):350–356. https://doi.org/10.1111/nph.18394.

Rutgers University. 2024. Tomatoes, p 443–464. In: Wyenandt A, Van Vuuren M (eds). Mid-Atlantic commercial vegetable production recommendations. Rutgers Univ Pub No. E001, Rutgers NJAES Cooperative Extension, New Brunswick, NJ, USA. https://njaes.rutgers.edu/pubs/publication.php?pid=E001.

Shen B-R, Wang L-M, Lin X-L, Yao Z, Xu H-W, Zhu C-H, Teng H-Y, Cui L-L, Liu E-E, Zhang J-J, He Z-H, Peng X-X. 2019. Engineering a new chloroplastic photorespiratory bypass to increase photosynthetic efficiency and productivity in rice. Mol Plant. 12(2):199–214. https://doi.org/10.1016/j.molp.2018.11.013.

South PF, Cavanagh AP, Liu HW, Ort DR. 2019. Synthetic glycolate metabolism pathways stimulate crop growth and productivity in the field. Science. 363(6422):eaat9077. https://doi.org/10.1126/science.aat9077.

South PF, Cavanagh AP, Lopez-Calcagno PE, Raines CA, Ort DR. 2018. Optimizing photorespiration for improved crop productivity. J Integr Plant Biol. 60(12):1217–1230. https://doi.org/10.1111/jipb.12709.

Stitt M. 1991. Rising CO2 levels and their potential significance for carbon flow in photosynthetic cells. Plant Cell Environ. 14(8):741–762. https://doi.org/10.1111/j.1365-3040.1991.tb01440.x.

Tripathi AD, Mishra R, Maurya KK, Singh RB, Wilson DW. 2019. Chapter 1 - Estimates for world population and global food availability for global health, p 3–24. In: Singh RB, Watson RR, Takahashi T (eds). The role of functional food security in global health. Academic Press, Cambridge, MA, USA. https://doi.org/10.1016/B978-0-12-813148-0.00001-3.

United Nations. 2024. World Population Prospects 2024: Summary of Results. UN DESA/POP/2024/TR/NO. 9. United Nations, New York, NY, USA. https://www.un.org/development/desa/pd/sites/www.un.org.development.desa.pd/files/files/documents/2024/Jul/wpp2024_summary_of_results_final_web.pdf.

Van Eck J, Keen P, Tjahjadi M. 2019. *Agrobacterium tumefaciens*-mediated transformation of tomato, p 225–234. In: Kumar S, Barone P, Smith M (eds). Transgenic plants: Methods and protocols. Springer, New York, NY, USA. https://doi.org/10.1007/978-1-4939-8778-8_16.

Whitney SM, Houtz RL, Alonso H. 2011. Advancing our understanding and capacity to engineer nature's CO2-sequestering enzyme, rubisco. Plant Physiol. 155(1):27–35. https://doi.org/10.1104/pp.110.164814.

Yadav S, Mishra A. 2020. Ectopic expression of C4 photosynthetic pathway genes improves carbon assimilation and alleviate stress tolerance for future climate change. Physiol Mol Biol Plants. 26(2):195–209. https://doi.org/10.1007/s12298-019-00751-8.

Zhang X-H, Webb J, Huang Y-H, Lin L, Tang R-S, Liu A. 2011. Hybrid Rubisco of tomato large subunits and tobacco small subunits is functional in tobacco plants. Plant Sci. 180(3):480–488. https://doi.org/10.1016/j.plantsci.2010.11.001.

Zhu X-G, Ort DR, Parry MAJ, von Caemmerer S. 2020. A wish list for synthetic biology in photosynthesis research. J Exp Bot. 71(7):2219–2225. https://doi.org/10.1093/jxb/eraa075.